Triplet Harvesting with 100% Efficiency by Way of Thermally Activated Delayed Fluorescence in Charge Transfer OLED Emitters

ARTICLE *in* ADVANCED MATERIALS · JULY 2013

Impact Factor: 17.49 · DOI: 10.1002/adma.201300753 · Source: PubMed

9 AUTHORS, INCLUDING:

Fernando Dias
Durham University
66 PUBLICATIONS **1,439** CITATIONS
SEE PROFILE

Konstantinos Bourdakos
University of Southampton
19 PUBLICATIONS **247** CITATIONS
SEE PROFILE

Jose Santos
Madrid Institute for Advanced Studies
21 PUBLICATIONS **394** CITATIONS
SEE PROFILE

Andy Monkman
Durham University
416 PUBLICATIONS **9,825** CITATIONS
SEE PROFILE

ADVANCED MATERIALS
www.advmat.de

Triplet Harvesting with 100% Efficiency by Way of Thermally Activated Delayed Fluorescence in Charge Transfer OLED Emitters

Fernando B. Dias, Konstantinos N. Bourdakos, Vygintas Jankus, Kathryn C. Moss, Kiran T. Kamtekar, Vandana Bhalla, José Santos, Martin R. Bryce, and Andrew P. Monkman*

The Holy Grail of organic light-emitting diodes (OLED) research has been the search for methods to overcome the limitation imposed by charge recombination spin statistics.[1] Upon charge recombination, three times more triplet excitons are generated than singlet excitons; therefore, the maximum internal efficiency of an OLED is limited to 25%,[2] unless methods to "harvest" the triplets, that is, convert them to emissive singlet states, are used.

Phosphorescent materials containing Ir(III), Pt(III), or other heavy metals can harvest both singlet and triplet excitons by means of enhanced intersystem crossing (ISC), via the heavy atom effect, and have been used widely to increase the emission yield to ≈100%.[3] However, these emitting complexes have to be dispersed in charge transporting matrices, and obtaining stable long-lifetime deep blue emitting phosphors has proved difficult and requires suitable high triplet level hosts.[3] Thus, deep blue, long lifetime phosphorescent OLEDs have not been demonstrated.

The use of triplet fusion (TF) has also been explored as an alternative approach to convert triplet into emissive singlet states. In this case, the maximum total singlet yield is limited to 62.5% and devices showing >40% TF contribution have been demonstrated, but the relative merit of this approach is still unsatisfactory.[4,5]

In the last year, a new triplet harvesting method that uses thermally activated up-conversion of triplet into singlet states has been shown, giving thermally activated delayed fluorescence (TADF), with no need of phosphorescent materials, and the possibility of obtaining blue emitters, that give very high total singlet yields.[6,7]

Dr. F. B. Dias, Dr. K. N. Bourdakos, Dr. V. Jankus, Prof. A. P. Monkman
Durham University
Physics Department
Rochester Building, South Road, DH1 3LE, UK
E-mail: f.m.b.dias@durham.ac.uk
Dr. K. C. Moss, Dr. K. T. Kamtekar, Dr. V. Bhalla, Dr. J. Santos, Prof. M. R. Bryce
Chemistry Department
Durham University
South Road, DH1 3LE, UK
Dr. V. Bhalla
Department of Chemistry
Guru Nanak Dev University
Amritsar 143005, India

DOI: 10.1002/adma.201300753

TADF or E-type delayed fluorescence[8] is directly proportional to the energy gap between the triplet and singlet states, ΔE_{ST}, which is governed by the electron exchange energy. In order to maximize TADF, ΔE_{ST} should be minimized. As predicted by Beens and Weller,[9] intramolecular charge transfer states (ICT) where the electron and hole are decoupled on different orbitals have zero exchange energy to first order giving rise to E-type delayed fluorescence.[10] There are theoretical reports that even claim that in many cases the singlet ^{1}CT state can lie below the triplet ^{3}CT.[11]

Using ICT emitters, Adachi and co-workers have shown that TADF can greatly enhance OLED efficiency,[6,7] and internal efficiencies up to a point near 100% have been reported.[12] Surprisingly, the ΔE_{ST} gap measured for most of these systems is much greater than the expected difference between the singlet and triplet CT states in a simple ICT system (<100 meV) to yield efficient TADF. For example, in a series of materials containing electron donor (D) and electron acceptor (A) units, and D-A-D structures, showing ΔE_{ST} from 0.32 to 0.54 eV, and efficient TADF in the blue spectral region,[7] the authors tentatively describe the origin of TADF to a mechanism that involves reverse internal conversion (RIC), from the donor centred $^3\pi\pi^*$ lowest triplet state to the ^{3}CT, followed by reverse intersystem crossing (RISC) to the ^{1}CT emissive state. However, the total energy gap between the lowest singlet ^{1}CT and triplet $^3\pi\pi^*$ states is still surprisingly high in order to give TADF, when compared with the 25 meV kT value at room temperature. Moreover, in related exciplex systems, a lower lying $^3\pi\pi^*$ than the ^{3}CT state quenches TADF, but does enhance total fluorescence efficiency by an enhanced contribution from TF.[13] Only when both D and A triplet levels are higher in energy than the CT state is TADF observed.[12]

Here, we show, by detailed spectroscopic measurements on a family of ICT materials, that even with such large ^{1}CT–$^3\pi\pi^*$ gaps, ΔE_{ST} > 0.3 eV, 100% TADF efficiency is achievable. We established that the energy levels involved are more complex than previously appreciated, with heteroatom lone pair orbitals playing a key role in this process.

A systematic series of D-A-D and D-D-D materials were synthesized, comprising five different core units (**1** to **5**) substituted with different electron donor units (**a** to **e**), see **Scheme 1**.

We elucidate a general mechanism governing the observation of TADF in these types of materials. Triplet state harvesting with 100% efficiency is observed, giving indication that efficient TADF can be obtained in many ICT materials, having appropriate groups containing heteroatoms in their structure.

ADVANCED MATERIALS
www.advmat.de

www.MaterialsViews.com

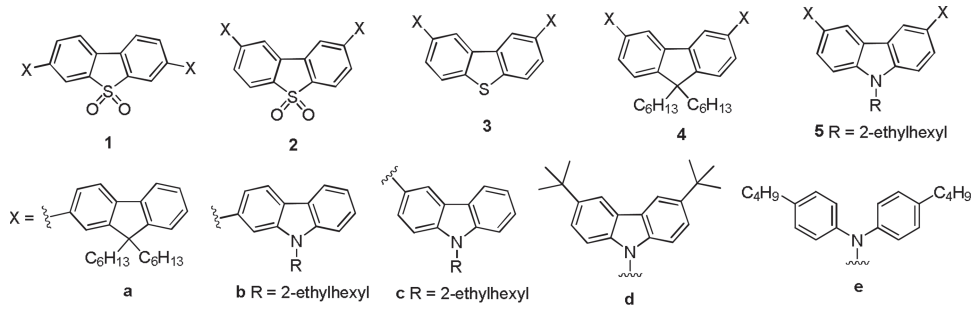

Scheme 1. Chemical structures and nomenclature of compounds used in this study.

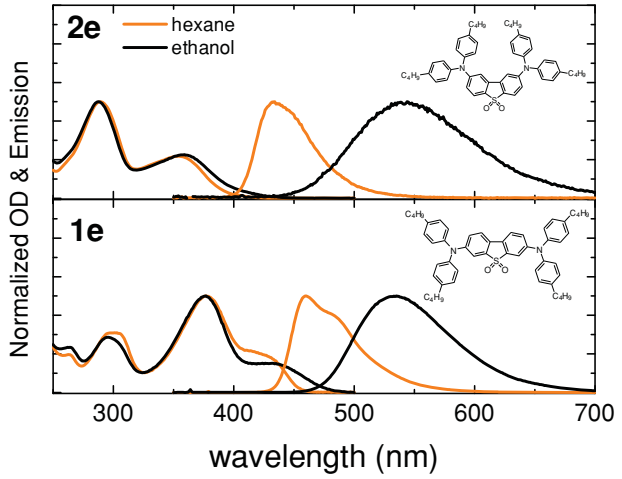

Figure 1. Absorption and emission spectra of compounds **2e** and **1e** in hexane and ethanol solutions. Both compounds show pronounced solvatochromism, with emission in the polar solvent (ethanol) appearing from a singlet excited state with charge transfer character.

Our materials show strong, well resolved emission in non polar solvents, assigned to an excited state with strong $^1\pi\pi^*$ character. In polar solvents, the emission appears broad and red-shifted, and is assigned to an excited state with strong intramolecular charge transfer character (^{1}CT).[14,15] **Figure 1** shows the absorption and emission spectra of compounds **1e** and **2e** in non-polar hexane and polar ethanol as examples. The spectra of all the other materials are given in Supporting Information (S2).

Well resolved phosphorescence, assigned to a triplet state with $^3\pi\pi^*$ character, see Supporting Information (S4), is observed below 100 K, independent of the solvent polarity for all materials. Interestingly, a clear pattern emerges when the relative phosphorescence intensity is compared for different materials, see **Figure 2** and Figure S3 in Supporting Information.

When the acceptor unit is "angularly" disubstituted (i.e., at the C-2,8 positions for dibenzothiophene-*S,S*-dioxide and dibenzothiophene; at the C-3,6 positions for fluorene and carbazole) and heteroatoms (nitrogen or oxygen) are present in the molecular structure, strong phosphorescence emission is observed at low temperatures. This emission is so strong that it can be easily observed with a normal spectrofluorimeter. However, when the acceptor unit is "linearly" disubstituted (i.e., at the C-3,7 positions for dibenzothiophene-*S,S*-dioxide and dibenzothiophene), phosphorescence is very weak. This effect is independent of the acceptor and donor units that have been used.

The energy differences (ΔE_{ST}) between the $E_{0\text{-}0}$ (^{1}CT) and the $E_{0\text{-}0}$ ($^3\pi\pi^*$) states are given in **Table 1**. In general, the "angular" disubstitution shifts the $^3\pi\pi^*$ triplet state to higher energies and smaller ΔE_{ST} energy gaps are obtained. However, the observation of strong phosphorescence is not correlated in a simple manner with the ΔE_{ST} energy gap. As examples, Figure 2 shows

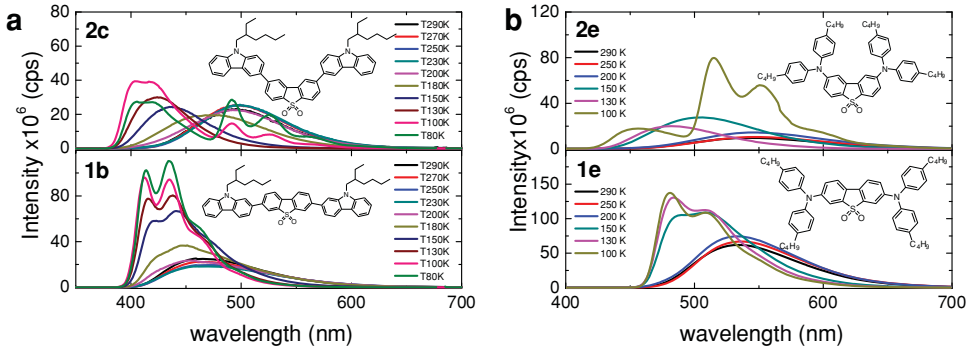

Figure 2. Emission spectra in ethanol as a function of temperature. a) compounds **1b** and **2c**, b) compounds **1e** and **2e**. The only difference between compounds **1b**/**2c** and compounds **1e**/**2e** are the positions where the dibenzothiophene-*S,S*-dioxide acceptor is substituted. Materials substituted at the 2,8-positions (**2c**/**2e**) show stronger phosphorescence emission at low temperatures, compared to the isomers **1b**/**1e**.

Adv. Mater. **2013**,
DOI: 10.1002/adma.201300753

Table 1. Excited state energies.

compound		Energy [eV]			
code	substitution	$^1\pi\pi^*$	^{1}CT	$^3\pi\pi^*$	ΔE_{ST}
1a	2-[3,7]-2′	3.33 ± 0.02	3.21 ± 0.02	2.22 ± 0.02	0.99 ± 0.04
1b	2-[3,7]-2′	3.26 ± 0.02	3.12 ± 0.03	2.28 ± 0.02	0.84 ± 0.05
1c	3-[3,7]-3′	3.27 ± 0.02	3.06 ± 0.03	2.29 ± 0.04	0. 77 ± 0.07
1d	9-[3,7]-9′	3.16 ± 0.02	2.95 ± 0.02	2.40 ± 0.02	0.55 ± 0.04
1e	N-[3,7]-N′	2.95 ± 0.02	2.74 ± 0.02	2.11 ± 0.04	0.63 ± 0.06
2a	2-[2,8]-2′	3.68 ± 0.02	3.37 ± 0.02	2.41 ± 0.02	0.96 ± 0.04
2c	3-[2,8]-3′	3.54 ± 0.02	3.11 ± 0.03	2.53 ± 0.02	0.58 ± 0.05
2d	9-[2,8]-9	3.26 ± 0.02	2.98 ± 0.02	2.63 ± 0.02	0.35 ± 0.04
2e	N-[2,8]-N′	3.15 ± 0.02	2.87 ± 0.03	2.39 ± 0.02	0.48 ± 0.05
3d	N-[2,8]-N′	3.59 ± 0.02	3.54 ± 0.03	2.97 ± 0.02	0.57 ± 0.05
4a	2-[3,6]-2′	3.75 ± 0.02	-	2.65 ± 0.04	1.1 ± 0.1
4d	9-[3,6]-9	3.63 ± 0.02	3.69 ± 0.02	2.82 ± 0.02	0.87 ± 0.04
5d	9-[3,6]-9	3.34 ± 0.02	-	2.88 ± 0.02	0.46 ± 0.04

the emission spectra of **2c**/**1b** and **2e**/**1e** in ethanol as a function of temperature. The first pair has ΔE_{ST} of 0.58 ± 0.05 eV and 0.84 ± 0.05 eV, and the second pair has 0.48 ± 0.05 eV and 0.63 ± 0.06 eV respectively. While only weak phosphorescence is observed from **1b** and **1e**; for **2c** and **2e** strong phosphorescence is observed. However, in the case of **4d**, and this is particularly interesting: even with ΔE_{ST} of 0.87 ± 0.04 eV strong phosphorescence is observed.

The observation of stronger phosphorescence in the "angularly" disubstituted materials correlates well with the observation of both lower fluorescence yield (Φ_F) and short $^1\pi\pi^*$ excited state lifetime, relative to their linearly disubstituted counterparts, (Supporting Information, S6). This indicates that the triplet yield is higher in the angular materials, relative to their linear analogues.

We have found in previous work that the excited state of the angular materials has stronger charge transfer character than the excited state of their linear analogues,[15] and that, in general, enhanced charge transfer character of the lowest singlet excited state favors higher intersystem crossing yields.[16] However, the observation of strong phosphorescence in compound **5d** which has no ICT character and in compound **2a**, see Supporting Information (S3), shows that it is the simultaneous presence of heteroatoms and the substitution at positions C-3,6 of the carbazole core and 2,8 of the dibenzothiophene-dioxide core (i.e., angular), instead of just the ICT nature of the excited state that is responsible for the observation of strong phosphorescence.

The lack of strong phosphorescence in compound **4a**, which is also angularly substituted, further reinforces the conclusion that the simultaneous presence of angular substitution, and groups containing heteroatoms is necessary to observe strong phosphorescence. In other words, the angular substituted materials containing nitrogen and oxygen atoms show, in general, stronger electronic coupling between the singlet and triplet excited states than their linear counterparts.

The requirement that groups containing heteroatoms in the chemical structure are necessary for the observation of strong phosphorescence implicates the involvement of triplet states with $^3n\pi^*$ character in the intersystem crossing mechanism. In fact, carbazole containing materials are known to have $n\pi^*$ transitions.[17] Moreover, Brunner, van Dijken, and co-workers have shown that the angular substitution of carbazole containing materials reduces the ST exchange energy relative to their linear counterparts.[18,19] This effect is attributed to a stronger localization of the triplet state, which raises its energy, while in linear carbazole substituted materials the triplet is more delocalized, and therefore of lower energy.[20] Both conditions, the presence of $n\pi^*$ transitions and smaller ST gaps, concur to the observation of stronger phosphorescence in the angularly substituted materials.

All compounds studied here show strong delayed fluorescence in degassed ethanol solution, with clear intramolecular origin for **2d** and **2e**. In these two cases, TADF is evident by the linear dependence of the log-log plot of DF intensity with excitation dose, see Supporting Information (S8). However, for other materials, a squared dependence of the DF intensity with excitation dose is observed (Supporting Information, S11), clearly indicating that TF dominates the production of DF. Complete DF quenching is observed under O_2 saturated conditions and, thus, the origin of the DF is clearly assigned to processes involving triplet states.[7,21]

DF intensity is found to increase with temperature in all materials studied (see **Figure 3** and Supporting Information), confirming a thermally activated step in RISC ($T_1 \rightarrow S_1$) irrespective of the magnitude of ΔE_{ST}. Moreover, the delayed emission appears with the same spectral distribution as the normal fluorescence but with a much longer decay time constant (equal to the feeding T_1 lifetime).[22]

We find that TADF and TF coexist in many of our materials (Supporting Information, S15), with the contribution of each mechanism depending on 1) the electronic coupling between

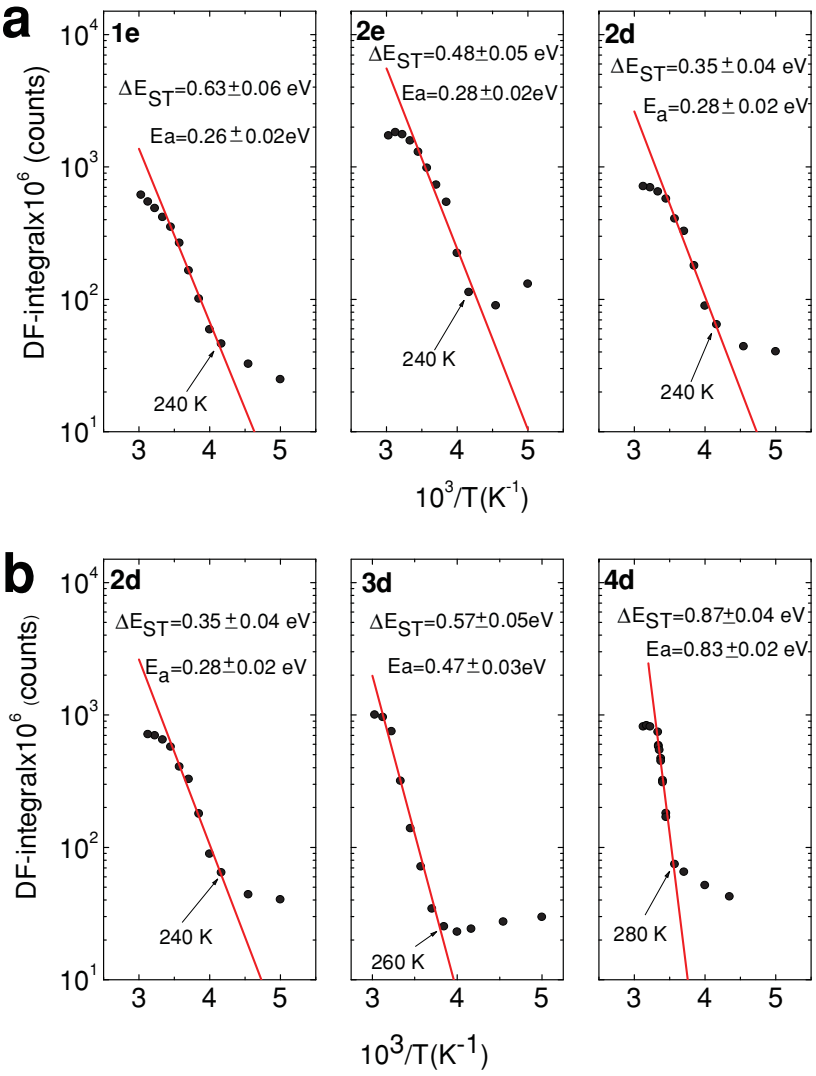

Figure 3. Arrhenius type plot of the temperature dependence of the delayed fluorescence. a) Compounds **1e**, **2e**, and **2d** have the same dibenzothiophene-dioxide acceptor core, but different donor units and structure. b) Compounds **2d**, **3d**, and **4d** have exactly the same donor units and structure, but different acceptor cores.

the singlet and the lowest triplet excited states, that is, if compounds are angularly substituted (strong coupling) or linearly substituted (weak coupling) and 2) the ST energy gap.

Compound **1b** with a large ^{1}CT–$^3\pi\pi^*$ (ΔE_{ST}) gap and weak coupling yields "pure" TF. However, **1e** still with weak coupling but smaller ΔE_{ST} (0.63 eV), shows more pronounced contribution from TADF. Compounds **2e** and **2d**, with smaller ΔE_{ST} gap and strong coupling give TADF.

Interestingly, with the exception of **1b**, which gives pure TF, the energy barrier and the turn on temperature for TADF, determined from a simple Arrhenius type plot, are the same for materials **1e**, **2e**, and **2d**, which have the same acceptor, and therefore the relative energy positions of the CT state and the lowest triplet states should be similar (see Figure 3a).

For materials with different acceptors, therefore different (higher) CT energies, and larger ΔE_{ST}, but still with strong coupling, that is, angularly substituted, the contribution from TADF is still very clear. However, the turn-on temperature for TADF is now higher: 260 K for **3d** (ΔE_{ST} = 0.57 eV) and 280 K for **4d** (ΔE_{ST} = 0.87 eV), and the TADF energy barriers are also higher, 0.47 eV for **3d** and 0.83 eV for **4d** (see Figure 3b).

The energy barrier E_a, obtained from the Arrhenius plot for the onset of TADF, and temperature threshold for the TADF contribution are therefore not related in a simple manner with the singlet-triplet energy splitting (ΔE_{ST}). Clearly, in the case of materials **1e** (ΔE_{ST} = 0.63 eV; E_a = 0.26 eV), **2e** (ΔE_{ST} = 0.48 eV; E_a = 0.28 eV), and **2d** (ΔE_{ST} = 0.35 eV; E_a = 0.28 eV), which have the same acceptor unit, and different S–T energy splitting, the energy barrier for thermally assisted RISC is independent of the magnitude of the S–T energy gap. Therefore, we propose that a middle gap state is present, which facilitates RISC to the ^{1}CT state. We note that materials **3d** (ΔE_{ST} = 0.57 eV; E_a = 0.47 eV) and **4d** (ΔE_{ST} = 0.87 eV; E_a = 0.83 eV), which have the same donor as material **2d**, but different acceptors show an energy barrier for thermally DF closer to the magnitude of their S–T energy splitting. This is particularly true for **4d** where no heteroatoms are present in the acceptor unit. Comparing materials **2d**, **3d**, and **4d**, all with the same structure and donor units, but different acceptors, strongly suggests that the inferred middle-gap state is associated with the dibenzothiophene-*S*,*S*-dioxide acceptor, and not with the donor carbazole unit.

In the case of materials showing pure TADF, the thermal activation energy barrier of the DF (ΔE_a^{TADF}), the triplet yield (Φ_T) and the rate constant for $S_1 \leftarrow T_1$ reverse intersystem crossing (k_{RISC}^{-T}) are obtained from fitting the integrated DF emission (I_{DF}) as a function of temperature, between 200 K and 330 K, with Equation 1 (see **Figure 4** and Figure S9 in the Supporting Information for more details). I_{PF} and I_{DF} are the intensities of prompt and delayed fluorescence respectively, k_P is the phosphorescence decay rate constant, and k_G^T is the triplet nonradiative decay rate constant.[23]

$$I_{DF} = \frac{I_{PF}}{A_2 + A_3\, e^{A_4 T^{-1}}} \quad (1)$$

where $A_2 = (\frac{1}{\Phi_T} - 1)$, $A_3 = \frac{k_P + k_G^T}{\Phi_T k_{RISC}^{-T}}$, and $A_4 = \frac{\Delta E_G^{TADF}}{R}$ are fitting parameters.

The terms $\frac{k_P + k_G^T}{\Phi_T k_{RISC}^{-T}}$ and Φ_T are assumed to be essentially independent of temperature, within the temperature range where ΔE_{ST} is determined (from 300 K to 200 K).

Excellent control over the fitting parameters is achieved through independent determination of key parameters over the

Adv. Mater. 2013,
DOI: 10.1002/adma.201300753

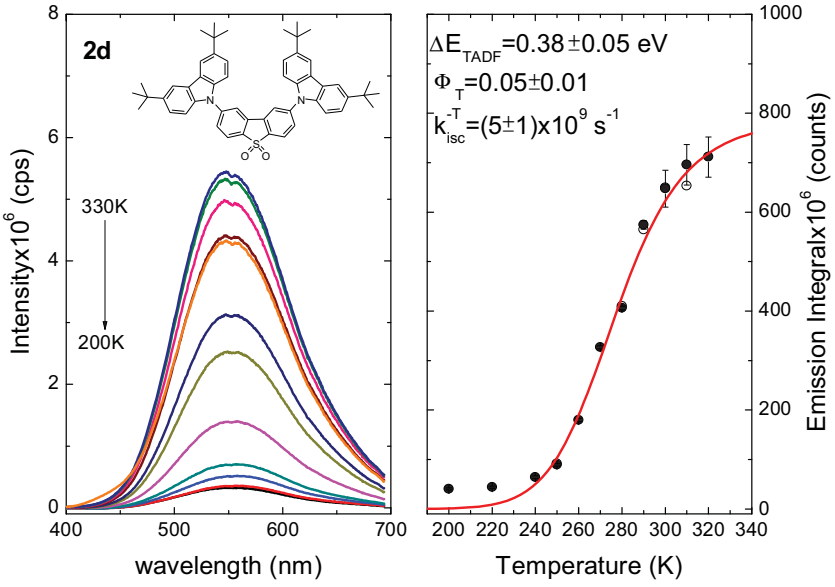

Figure 4. DF emission as a function of temperature for compound **2d**. The DF emission decreases with decreasing temperature (left), confirming the thermally assisted mechanism. Fitting the DF integral with Equation 1 (red line), allows the determination of the energy barrier for up-conversion of triplet into singlet states (ΔE_a^{TADF}), the triplet yield (Φ_T) and the reverse intersystem crossing rate (k_{RISC}^{-T}).

measured temperature range. The prompt fluorescence (I_{PF}) and its lifetime are essentially independent of temperature in the 300 K to 200 K interval (see Supporting Information, S10).

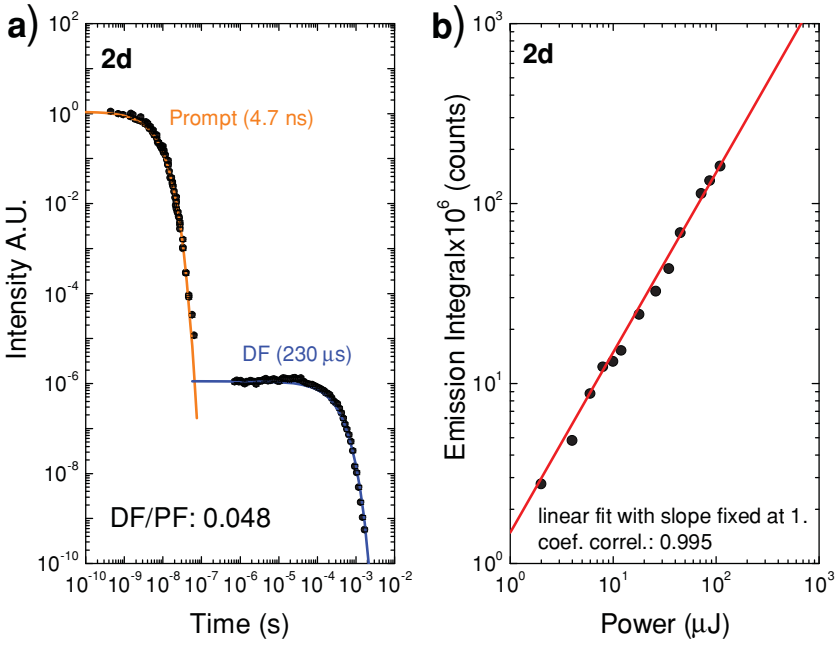

Figure 5. a) Prompt (PF) and delayed (DF) fluorescence collected in a single experiment in a time interval spanning 9 orders of magnitude. PF and DF follow clear exponential decay laws, allowing a simple determination of the DF/PF ratio and lifetimes in a single experiment. b) Variation of DF intensity with excitation dose. A clear linear dependence is observed throughout the entire excitation range, showing the pure thermally assisted nature of the TADF mechanism in **2d**.

This also gives additional support to the temperature independence of $\frac{k_P+k_G^T}{\Phi_T k_{RISC}^{-T}}$ and Φ_T as stated before.

I_{PF} is determined experimentally at room temperature from a plot of the emission intensity over 9 decades of time (see **Figure 5**a), allowing the collection in the same single experiment of both I_{PF} and I_{DF}. From this plot the I_{DF}/I_{PF} ratio and the DF lifetime are determined, and lower and higher limits established for $A_2 = \left(\frac{1}{\Phi_T} - 1\right)$ and $A_3 = \frac{k_P+k_G^T}{\Phi_T k_{RISC}^{-T}}$.

The I_{DF}/I_{PF} ratio is related to Φ_T by Equation 2, where Φ_S is the yield of singlet formation through RISC. Since Φ_S has to be less than or equal to 1, a lower limit for Φ_T is given by $\frac{I_{DF}}{I_{DF}+I_{PF}}$, and the maximum value Φ_T can achieve is $(1 - \Phi_F)$, therefore $A_2 = \left(\frac{1}{\Phi_T} - 1\right)$ can only take values between $\left(\frac{1}{1-\Phi_F} - 1\right)$ and $\frac{I_{PF}}{I_{DF}}$.[23]

$$\frac{I_{DF}}{I_{PF}} = \frac{1}{\frac{1}{\Phi_T \Phi_S} - 1} \quad (2)$$

The parameter A_3 is related to the triplet lifetime and, thus, the DF lifetime, which is determined from the time dependence of the emission intensity. A good estimate of its value is therefore obtained by measuring the DF lifetime, on the order of 10^{-4} s in our materials (see Figure 5a), and using the expected order of magnitude of k_{RISC}^{-T}, 10^7 s^{-1} (for C_{70},[23] and 10^8 s^{-1} for eosin,[24]) A_3 can thus vary between 10^{-8} and 10^{-3}.

Finally, (ΔE_a^{TADF}) cannot be larger than the singlet ^{1}CT-triplet $^3\pi\pi^*$ energy splitting (ΔE_{ST}), which is determined experimentally from fluorescence and phosphorescence emission spectra. Within these limits robust fits of the DF emission integral as a function of temperature are obtained for TADF materials.

As mentioned earlier, strickly linear dependence of the DF intensity integral with excitation dose is observed for compounds **2d** and **2e** (see Figure 5b), confirming the intramolecular origin of TADF mechanism in these two materials and the apropriateness of Equation 1 to fit the data.

Table 2 shows the results obtained with three representative materials, selected with the same acceptor, dibenzothiophene-*S*,*S*-dioxide, and organized by increasing charge transfer character of their lowest excited state ^{1}CT. This has been evaluated from the Stokes shift in solvents with different polarity and TD-DFT calculations (see S13 in Supporting Information).[15]

The increasing triplet yield and decreasing fluorescence yield, observed from **1e** to **2d**,

Table 2. Photophysical parameters obtained from selected materials.

code	Φ_F (±0.05)	ΔE_{ST}	ΔE_a^{TADF} [eV]	Φ_T	$k_{RISC}^{-T} \times 10^9$ [s^{-1}]	Power dependence	DF
1e	0.6	0.63 ± 0.06	0.36 ± 0.05	0.003 ± 0.001	2 ± 1	2.0	TF[a)]
2e	0.3	0.48 ± 0.05	0.36 ± 0.05	0.03 ± 0.01	0.9 ± 0.1	1.0	TADF
2d	0.26	0.35 ± 0.04	0.38 ± 0.05	0.05 ± 0.01	5 ± 1	1.0	TADF

[a)]Strictly speaking, Equation 1 is not applicable to **1e**, since TF dominates the observation of DF.

and the variation of the triplet yield throughout is clearly correlated with the increasing charge transfer character of the lowest singlet excited state ^{1}CT. This is in agreement with our previous work,[16] and also with reports from others.[25]

The RISC rate constant (k_{RISC}^{-T}), determined from A_3 and the DF lifetime, show values varying around 10^9 s^{-1}. The process of thermal activation from "a triplet state" to the ^{1}CT singlet state, involves the population of upper vibrational levels of the triplet manifold, followed by reverse intersystem crossing. In this way, k_{RISC}^{-T}) is the average rate constant for the adiabatic $S_1 \leftarrow T_1$ intersystem crossing step.[24] Our results are in excellent agreement with determinations of this rate constant from previous studies on different materials.[23,24,26]

The energy barrier for thermally activated DF (ΔE_a^{TADF}) in the materials shown in Table 2 is found to be around 0.36 ± 0.05 eV, and this is independent of the substitution position, type of donor unit, and degree of charge transfer, in agreement with the independent determination done in the previous section. Clearly, the dominant RISC step arises from a triplet state which is not the ^{3}CT state nor the $^3\pi\pi^*$ state. In these materials, the ΔE_{ST} energy ranges from 0.35 ± 0.04 eV to 0.63 ± 0.05 eV, whereas the energy barrier for TADF shows only small variations around 0.36 eV, much smaller than the ΔE_{ST}. Therefore, the triplet states that are being converted to singlet states in the TADF mechanism cannot be the lowest $^3\pi\pi^*$ as was initially proposed.[7] Another long lived triplet state must therefore be present in these materials; otherwise, the observation of TADF with a energy barrier smaller than the ΔE_{ST} energy gap cannot be possible.

Triplet states with $n\pi^*$ character are known to exist in compounds with heteroatoms, as for example compounds containing carbonyl, nitro, diazo, thiol, and similar groups[27] as well as carbazole,[17] and, therefore, we propose that this is the "new" triplet state here.

The presence of triplet states, involving nonbonding electrons, has been proposed previously to explain the observation of much higher relative quantum yields of phosphorescence, compared with fluorescence, in compounds containing sulfur.[28] The marked variation of the intersystem crossing rate with the $-NO_2$ substitution in mononitro-pyrenes, has also been explained by the existence of an upper triplet state, with $^3n\pi^*$ character, that acts as an intermediary receiver state.[29] In general, the efficient intersystem crossing in nitroaromatic compounds is also explained by the strong electronic coupling between the $^1\pi\pi^*$ lowest singlet excited state (S_1) and the upper triplet states with $^3n\pi^*$ character.[30]

Moreover, in a recent paper, Estrada and co-workers have proposed the presence of a triplet state with $n\pi^*$ character to explain the enhanced intersystem crossing in angularly disubstituted carbazole-fluorenone-carbazole oligomer.[31]

Further evidence for the presence of $^3n\pi^*$ states in our systems is obtained by comparing the DF intensity in compounds **4a** and **5d**. The lowest singlet excited state in these two compounds has no ICT character. However, the intensity of the delayed emission is clearly higher in **5d**, where nitrogen lone pairs are present; see Supporting Information, S14. Furthermore, while **5d** shows strong phosphorescence at low temperatures, in **4a** no phosphorescence is observed, despite both materials being angularly substituted.

Given the above evidence in our materials for the role of a $^3n\pi^*$ state, which acts as a receiver triplet state, and gives the invariant energy barrier for TADF, we construct an energy level system shown in **Figure 6**.

The $^3n\pi^*$ triplet receiver state plays a critical role in the TADF mechanism. In agreement with El-Sayed's rules for intersystem radiationless transitions of the type $^1n\pi^*$ $^3\pi\pi^*$ or $^1\pi\pi^*$ $^3n\pi^*$,[27] the intersystem crossing from the ^{1}CT singlet state directly to the $^3n\pi^*$ triplet receiver state is more efficient than the ISC from ^{1}CT to the lower lying $^3\pi\pi^*$ triplet state (consistent with a greater Frank-Condon weighted density of states overlap). This means that the lowest $^3\pi\pi^*$ triplet state will be populated via the $^3n\pi^*$ triplet receiver state, itself populated from the ^{1}CT state or, more probably, via the ^{3}CT by internal conversion. The presence of the $^3n\pi^*$ state explains, therefore, the enhanced triplet formation yield observed in all the angularly substituted materials when compared with compound **4a**. Note, however, that

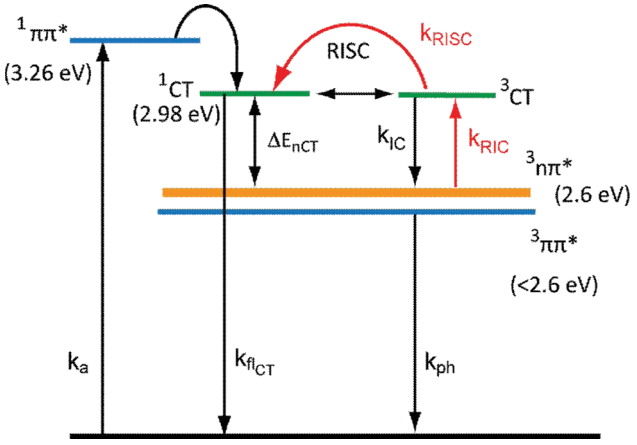

Figure 6. Energy level diagram showing the relevant photophysical processes to support the observation of TADF. The energies given are for compound **2d**.

Adv. Mater. **2013**,
DOI: 10.1002/adma.201300753

the ISC between ^{1}CT and ^{3}CT states should be more efficient than between ^{1}CT and the triplet ^{3}nπ^*, and between ^{1}CT and the triplet $^3\pi\pi^*$. Otherwise, the fluorescence yield of all materials, linear and angularly substituted, would be much weaker. The vanishingly small energy gap between ^{1}CT and ^{3}CT excited states, therefore, plays a fundamental role on the population of the lower lying triplet states, ^{3}nπ^* and $^3\pi\pi^*$, which occurs predominantly through internal conversion from the ^{3}CT state.

In our materials set, RISC can however occur in two different ways depending on the energy gap between the $^3\pi\pi^*$ and ^{3}nπ^* triplet states. When this gap is small, the situation observed in compounds **2d** and **2e**, RISC occurs by a purely thermally assisted mechanism; a first step involves successive reverse internal conversion between the $^3\pi\pi^*$, ^{3}nπ^*, and ^{3}CT, followed by reverse intersystem crossing between the ^{3}CT and the ^{1}CT states. This is demonstrated by the linear power dependence of the DF emission integral, see Table 2, Figure 5b, and Supporting Information, S8–S11, and can be truly called "TADF". We note that 0.36 eV is less than two carbon double bond vibrational quanta and may give insight into how it is relatively easy to cross such a large energy barrier.

When the energy gap between the $^3\pi\pi^*$ and ^{3}nπ^* triplet states is large, the situation observed in compounds **1e** and **1b**, or when no ^{3}CT state is present, the case of **5d**, the reverse intersystem crossing mechanism cannot occur by this pure thermally assisted mechanism alone. Now a first step that involves triplet fusion is necessary to populate either the ^{3}nπ^* triplet receiver state, which is then followed by thermal assisted RIC and RISC between the ^{3}CT and the ^{1}CT states, mediated by hyperfine interactions. Or, more likely given the magnitude of twice the $^3\pi\pi^*$ energy (> energy of the $^1\pi\pi^*$) the TF directly generates singlet states in the classical manner[13] with a smaller TADF contribution at high temperatures, see Supporting Information, S15. The dominance of the TF step is demonstrated by the squared power dependence of the DF emission integral observed for compounds **5d**, **1e**, and **1b** (S8-S11, Supporting Information). Which mechanism dominates, TADF or TF, is found to be dependent on ΔE_{ST} and the electronic coupling between the ^{3}CT and the ^{3}nπ^* states, that is, if compounds are angular (strong coupling) or linear (weak coupling).

The observation of thermally activated DF in compound **1b** is particularly striking. This material has ΔE_{ST} = 0.84 eV, and DF can be observed even at 100 K in competition with the phosphorescence from the $^3\pi\pi^*$ triplet state (S13, Supporting Information). The DF emission in **1b** decays with two time constants, giving clear indication for RISC involving two distinct triplet states that are feeding the singlet excited state, see Supporting Information, S11. In **1b**, the energy gap between the lowest $^3\pi\pi^*$ triplet state and the ^{3}nπ^* triplet state is sufficiently large (>0.5 eV), to allow the interconversion steps between the lowest triplet ($^3\pi\pi^*$) state and the ^{3}nπ^* state, and between the ^{3}nπ^* and the ^{1}CT singlet state to be distinguished.

The observation of a squared dependence of the DF intensity with excitation dose in **5d**, highlights the role of reverse internal conversion between the ^{3}nπ^* and the ^{3}CT triplet states in the TADF mechanism. Compounds **5d** and **2e** have similar ΔE_{ST}, but while **2e** has ICT character, **5d** has a D–D–D structure, not D–A–D, and consequently no ICT character is observed. **2e** shows pure thermal assisted RISC, with strictly linear TADF intensity with excitation dose, **5d** shows a squared dependence. For **5d**, RISC occurs directly from the $^3\pi\pi^*$ or from the ^{3}nπ^* to the $^1\pi\pi^*$ singlet state, and thus spin flip is required within the transition covering the 0.48 eV energy gap. This is facilitated when two triplet states interact under TF. For **2e**, the transition between the ^{3}nπ^* to the ^{3}CT does not involve spin flip, which rapidly occurs between the ^{3}CT→^{1}CT transition, efficiently facilitated by the smaller energy gap between these two states and strong hyperfine interactions.

In the **2d** and **2e** compounds, which show pure thermal assisted RISC, the energy gap between the lowest $^3\pi\pi^*$ triplet state and the ^{3}nπ^* triplet state is small. The triplet yield determined from the fitting of the TADF temperature dependence with Equation 1, therefore represents the total amount of triplets that are formed. This is in contrast to what happens when TF is operative, where two triplets are necessary to form one singlet. The observation of a PF/DF emission ratio that is in excellent agreement with the triplet yield therefore gives strong indication that triplets are being harvest with efficiency close to 100% in these materials.

In **2d** and **2e**, the small ST energy gap (ΔE_{ST} < 0.5 eV), strong ICT character and small (<0.1 eV) energy gap between the lowest $^3\pi\pi^*$ and the ^{3}nπ^* triplet states, accounts for the observation of pure TADF mechanism with 100% triplet harvesting.

In summary, we have demonstrated that the material structure, that is, angular versus linear structures, the presence of a ^{3}nπ^* triplet state and charge transfer states with very small exchange energy are required to fully explain the observation of TADF in ICT materials with relatively large singlet ^{1}CT-triplet $^3\pi\pi^*$ energy splitting. This TADF mechanism is shown to be nearly 100% efficient at converting triplet to singlet states. In most materials the energy gaps are such that mixed TADF and TF emission is observed, usually dominated by the TF contribution. The key role of the ^{3}nπ^* can also explain the recent results of Adachi and co-workers[12] who demonstrate near 100% internal quantum efficiency in a device where the ^{3}CT state is higher in energy than the triplet energy of the host material used which should efficiently quench the ^{3}CT: however, the ^{3}nπ^* (and $^3\pi\pi^*$ states) will both be lower in energy than the host so avoiding quenching. We believe our results are quite general and can be directly applied to explain the observation of TADF in related molecular systems and can be used to guide the choice of new emitters.

Experimental Section

Solutions (10^{-5}–10^{-4} M) of all materials were degassed using 5 freeze/thaw cycles. Absorption and emission spectra are collected using a UV-3600 double beam spectrophotometer (Shimadzu), and a Fluorolog fluorescence spectrometer (Jobin Yvon). Time resolved fluorescence decays were collected using the picosecond time correlated single photon counting technique (impulse response function, IRF: 21 ps). The vertical polarization excitation source was the second-harmonic from a picosecond Ti:sapphire laser (Coherent). Emission was collected using a polarizer at magic angle and detected by a double subtractive monochromator, (Acton Research Corporation), coupled to a microchannel plate photomultiplier tube (Hamamatsu R3809U-50). Signal acquisition was performed using a TCSPC module (Becker & Hickl SPC-630). For longer time scales, a 405 nm diode laser (PicoQuant), with 40MHz repetition rate was used as the excitation source. Temperature

dependent measurements were acquired using a model liquid nitrogen cryostat (Janis Research). Phosphorescence, prompt fluorescence (PF), and delayed emissions (DF) spectra and decays were recorded using nanosecond gated luminescence and lifetime measurements (from 400 ps to 1 s) using a high energy pulsed Nd:YAG laser emitting at 355 nm (EKSPLA). Emission was focused onto a spectrograph and detected on a sensitive gated iCCD camera (Stanford Computer Optics) having sub-nanosecond resolution. PF/DF time resolved measurements were performed by exponentially increasing gate and delay times; details can be found elsewhere.[32]

Supporting Information

Supporting Information is available from the Wiley Online Library or from the author.

Acknowledgements

We thank the Royal Society (V.B.) and EPSRC (J.S., V.J.) for funding.

Received: February 15, 2013
Revised: April 19, 2013
Published online:

[1] S. R. Forrest, *Nature* **2004**, *428*, 911.
[2] M. A. Baldo, D. F. O'Brien, Y. You, A. Shoustikov, S. Sibley, M. E. Thompson, S. R. Forrest, *Nature* **1998**, *395*, 151.
[3] M. A. Baldo, S. R. Forrest, M. E. Thompson, in *Organic Electroluminescence* (Ed: Z. H. Kafafi) CRC press, Taylor & Francis Group, Boca Raton **2005**.
[4] D. Y. Kondakov, T. D. Pawlik, T. K. Hatwar, J. P. Spindler, *J. Appl. Phys.* **2009**, *106*, 124510.
[5] S. M. King, M. Cass, M. Pintani, C. Coward, F. B. Dias, A. P. Monkman, M. Roberts, *J. Appl. Phys.* **2011**, *109*, 074502.
[6] K. Goushi, K. Yoshida, K. Sato, C. Adachi, *Nat. Photonics* **2012**, *6*, 253.
[7] Q. Zhang, J. Li, K. Shizu, S. Huang, S. Hirata, H. Miyazaki, C. Adachi, *J. Am. Chem. Soc.* **2012**, *134*, 14706.
[8] C. A. Parker, C. G. Hatchard, *Trans. Faraday Soc.* **1961**, *57*, 1894.
[9] H. Beens, A. Weller, *Acta Phys. Polym.* **1968**, *34*, 593.
[10] B. Frederichs, H. Staerk, *Chem. Phys. Lett.* **2008**, *460*, 116.
[11] S. Difley, D. Beljonne, T. V. Voorhis, *J. Am. Chem. Soc.* **2008**, *130*, 3420.
[12] H. Uoyama, K. Goushi, K. Shizu, H. Nomura, C. Adachi, *Nature* **2012**, *492*, 234.
[13] V. Jankus, C. Chien-Jung, F. B. Dias, A. P. Monkman, *Adv. Mater.* **2013**, *25*, 1455.
[14] F. B. Dias, S. Pollock, G. Hedley, L. Pålsson, A. Monkman, I. I. Perepichka, I. F. Perepichka, M. Tavasli, M. R. Bryce, *J. Phys. Chem. B* **2006**, *110*, 19329.
[15] K. C. Moss, K. N. Bourdakos, V. Bhalla, K. T. Kamtekar, M. R. Bryce, M. A. Fox, H. L. Vaughan, F. B. Dias, A. P. Monkman, *J. Org. Chem.* **2010**, *75*, 6771.
[16] S. King, R. Matheson, F. B. Dias, A. P. Monkman, *J. Phys. Chem. B* **2008**, *112*, 8010.
[17] A. Kohler, H. Bassler, *Mater. Sci. Eng. R* **2009**, *66*, 71.
[18] K. Brunner, A. van Dijken, H. Borner, J. J. A. M. Bastiaansen, N. M. M. Kiggen, B. M. W. Langeveld, *J. Am. Chem. Soc.* **2004**, *126*, 6035.
[19] A. van Dijken, J. J. A. M. Bastiaansen, N. M. M. Kiggen, B. M. W. Langeveld, C. Rothe, A. Monkman, I. Bach, P. Stossel, K. Brunner, *J. Am. Chem. Soc.* **2004**, *126*, 7718.
[20] I. Avilov, P. Marsal, J. Brédas, D. Beljonne, *Adv. Mater.* **2004**, *16*, 1624.
[21] G. Méhes, H. Nomura, Q. Zhang, T. Nakagawa, C. Adachi, *Angew. Chem. Int. Ed.* **2012**, *124*, 11473.
[22] B. Valeur, *Molecular Fluorescence Principles and Applications*, Wiley-VCH, Weinheim **2002**.
[23] M. N. Berberan-Santos, J. M. M. Garcia, *J. Am. Chem. Soc.* **1996**, *118*, 9391.
[24] C. A. Parker, *Photoluminescence of Solutions*, Elsevier Publishing Company, Amesterdam **1968**.
[25] D. Veldman, S. M. A. Chopin, S. C. J. Meskers, R. A. J. Janssen, *J. Phys. Chem. A* **2008**, *112*, 8617.
[26] C. Baleizão, M. N. Berberan-Santos, *J. Chem. Phys.* **2007**, *126*, 204510.
[27] S. K. Lower, M. A. El-Sayed, *Chem. Rev.* **1966**, *66*, 199.
[28] R. S. Becker, A. D. Jordan, J. Kolc, *J. Chem. Phys.* **1973**, *59*, 4024.
[29] E. Plaza-Medina, W. Rodríguez-Córdoba, J. Peon, *J. Phys. Chem. A* **2011**, *115*, 9782.
[30] E. Collado-Fegoso, J. S. Zugazagoitia, E. Plaza-Medina, J. Peon, *J. Phys. Chem A* **2009**, *113*, 13498.
[31] L. A. Estrada, J. E. Yarnell, D. C. Neckers, *J. Phys. Chem. A* **2011**, *115*, 6366.
[32] C. Rothe, A. P. Monkman, *Phys. Rev. B* **2003**, *68*, 075208.